N. Taymourtash, V. Muscarello, G. Quaranta
Gust and Inflow Model Identification from Wind Tunnel Tests for Rotorcraft-Obstacle Interaction
in: 25th Conference of the Italian Association of Aeronautics and Astronautics (AIDAA 2019), Roma, Italy, 9-12 Sept. 2019, ISBN: 9788894396010, p. 1981-1989

Italian Association of Aeronautics and Astronautics
XXV International Congress
9-12 September 2019 | Rome, Italy

GUST AND INFLOW IDENTIFICATION FROM WIND TUNNEL TESTS FOR ROTORCRAFT-OBSTACLE INTERACTION

N. Taymourtash[1], V. Muscarello[2], G. Quaranta[3]

[1,2,3] Department of Aerospace Science and Technology, Politecnico di Milano

[1]Neda.Taymourtash@polimi.it [2]Vincenzo.Muscarello@polimi.it [3]Giuseppe.Quaranta@polimi.it

ABSTRACT

The present paper investigates the aerodynamic interaction of a helicopter and ship airwake exploiting wind tunnel data. A series of wind tunnel experiment, using a scaled helicopter model and Simple Frigate Shape 1, has been performed to measure forces and moments acting on the rotor, while the helicopter is approaching the flight deck. With the rotor positioned at the starting point of the landing trajectory, the load measurements are used to modify the distribution of the inflow over the rotor in multibody simulation environment, in order to generate same loads, including thrust, torque and in-plane moments. Then, an identification algorithm is developed to capture the effect of ship airwake on the rotor loads during the maneuvers, modeling it as an external gust to the rotor inflow. The gust velocity is obtained through an optimization algorithm with the objective of generating same load coefficients as the experiment. The simulation results show that the same load coefficients as the experiment can be generated by implementing a linear gust over the rotor with a magnitude that changes as the rotor moves through the wake of ship.

Keywords: Rotorcraft – Shipboard Operation- Wind Tunnel Experiment

1 INTRODUCTION

Helicopters are regularly required to perform challenging missions in confined areas and close to obstacles. Search and rescue missions over land and water, urban transport, intervention in natural disasters such as flooding or earthquake are some examples in which rotorcraft interacts with the surrounding environment. In these situations, performance and handling qualities of the rotorcraft are highly affected by the presence of the obstacles in close proximity. Offshore operations, like those involving rotorcraft, from and to moving decks and ships are among the most demanding tasks for pilots. In this case, due to the combination of moving flight deck, flying close to the ship hangar wall, changing speed and direction of the wind and turbulent ship airwake, pilot workload is significantly increased which may endanger the safety of flight. It has been shown that most of the frequency content of the unsteady airwake is concentrated in the range of 0.2-2 Hz [1]. This bandwidth covers the widely accepted range of pilot closed-loop control frequencies which is less than 1.6 Hz.

The complex aerodynamic environment under which such operations take place is expected to affect directly the handling qualities, and so pilot workload and safety of operation. Analysis of safety operating limits for such demanding missions needs a series of flight test which are inherently hazardous and extremely expensive. Currently, those assessments are typically done only for the most demanding operations such as those of military helicopters operating on moving ships. Each combination of ship- rotorcraft should be tested for a range of wind speed and direction in order to find a safe flight envelope. Consequently, development of the helicopter-obstacle Dynamic Interface Simulation (DIS) is considered as a viable solution which reduces the cost and hazards of time-consuming at-sea test campaigns [2]. A better understanding of the environmental conditions could lead to the development of more accurate simulation environment for such demanding operation to improve pilot training. All those elements will contribute to the improvement of safety of rotorcraft operations, which is the objective of the NITROS project [3].

Regarding the complexity of the flow field generated by the rotorcraft-ship interaction, development of an appropriate airwake model which can capture the induced airloads of the rotor is of great importance. Various numerical or experimental approaches can be taken for airwake modelling which result in different levels of the simulation fidelity. The effect of coupling is worth to be considered in both numerical and experimental analysis of the shipboard operation. The most simplified approach is uncoupled simulation which means there is no interaction between rotorcraft and ship airwake. One-way coupling approach, which has been extensively implemented in simulation environments so far, accounts only for the effect of ship airwake on the rotor inflow [4]. However, since the airwakes and rotor dynamics are unsteady and nonlinear, the correctness of the overall solution obtained by the principle of superposition is highly questionable [5]. The more promising approach is two-way coupling or fully coupled simulation which includes mutual effect of the rotorcraft and ship airwake. In this approach, the CFD solver and flight dynamics simulation are run simultaneously with communication between two codes [6, 7, 8]. Depending on the computational cost of the numerical algorithm, this approach might be used in real time flight simulation. However, the results of coupled simulation need to be validated with experimental tests.

The approach taken in this research relies on wind tunnel experiments in order to improve the fidelity of flight dynamics simulation. This is the first step towards development of a fully coupled flight dynamics simulation with wind tunnel in the loop. To better understand the variables of the rotor response, a second-order quasi-steady approximation of the rotor dynamics can be considered:

$$D_2\ddot{\vec{q}} + D_1\dot{\vec{q}} + D_0\vec{q} = D_g\vec{u}_g + D_c\vec{u}_c \quad (1)$$

Here, $\vec{q}$ consists of all rotor states (including rigid and elastic states) and inflow variables. To incorporate the inflow variables into this model, the theory of dynamic inflow should be implemented which relates the airloads of the rotor to the induced-flow distribution over the rotor disk. Equation 1 clearly shows that the rotor loads are not only function of rotor states and inflow variables, but also affected by gust velocities. Consequently, it can be expected to reproduce the low-frequency contents of the rotor response (in terms of loads) by taking these two steps:

- Reconstructing the average and linear variation of the inflow
- Identifying a gust model that is representative of the unsteady wake caused by interaction with surrounding environments

This paper presents the identification of gust and inflow models, implementing an experimental database collected from wind tunnel tests. In the following section, the experimental setup will be briefly introduced. Then, the multibody approach used for modelling the rotor is explained. Finally, the identification algorithm along with the results are discussed.

2 WIND TUNNEL EXPERIMENT

Considering the shipboard operation as one of the most interactive missions which results in a complex flowfield that increases substantially the workload of the pilot, the experiment was designed to simulate a landing trajectory of a scaled helicopter on a generic ship. Since the details of the ship superstructure have not been considered interesting in this research, the Simple Frigate Shape 1 has been selected which is a highly simplified but representative ship geometry, developed as a part of an international collaboration in which Canada, Australia, UK and USA evaluated the ability of CFD codes to simulate complex airwakes [9]. This model has been scaled down with a geometric factor of 12.5 in order to have enough space on the flight deck for landing of the helicopter model. The experiments were conducted in the environmental test chamber of the Large wind tunnel of Politecnico di Milano (GVPM, see [10]). Taking advantage of the large test chamber (13.84 m wide, 3.84 m high and 38 m long), the geometric scale of 1:12.5 results in quite higher Reynolds Number compared with similar studies in the literature.

The helicopter model, which has already been exploited in previous wind tunnel investigations [11, 12], has four untwisted and untapered rectangular blades and a diameter of 0.75 m. A constant pitch angle of 10◦ was fixed in all tests, since the swashplate was not included in the current setup to trim the rotor. The rotational speed of the rotor was maintained in all tests by means of a brush-less low-voltage electrical motor with an electric controller. A Hall effect sensor with sampling frequency of one per revolution was implemented which acts as the feedback signal for RPM control. Forces and moments acting on the rotor have been measured for all points by implementing a six-components balance nested inside the fuselage. The helicopter model was mounted on a series of traversing guides so that its relative position with respect to the ship could be changed. The SFS1 model was instrumented with several pressure taps connected to pressure scanners and high-frequency pressure transducers, in order to allow for both steady and unsteady pressure measurements. PIV of the ship airwake and of the helicopter inflow were carried out in order to have a better understanding of how the interacting flow fields affected the helicopter performance. Figure 2 shows the setup of the experiment mounted inside the GVPM.

Figure 1: The test rig mounted inside the GVPM

In order to simulate the landing trajectory, the rotorcraft was positioned in a series of points representative of a typical fore-aft landing trajectory and aerodynamic loads generated by the rotor were measured. The trajectory, as shown in Figure 3, consists of five points (P1 to P5) that can be divided into two distinctive segments: the initial phase in which the helicopter approaches the flight deck from stern side along the centerline of the flight deck and the descent phase, i.e. an oblique path towards landing spot, which is considered close to the centre of the flight deck. Furthermore, three additional points above the landing point have been selected in order to simulate a vertical descent (P5 to P8). The reference frame shown in Figure 3 refers to the rotor reference frame whose x axis (Xr) is nose to tail, vertical axis is bottom to top (Zr) and lateral axis is toward the advancing side of the rotor plane.

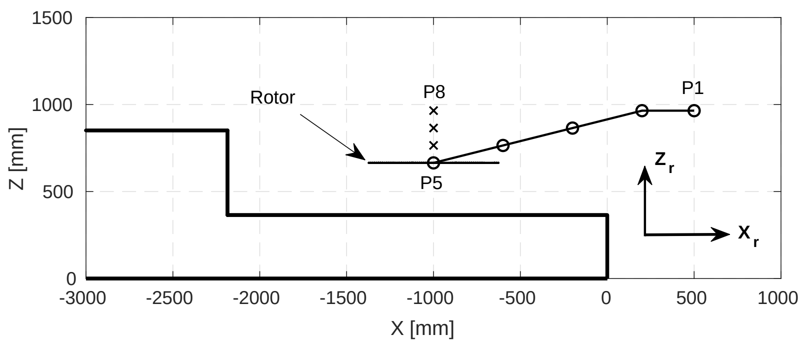

Figure 2: Side-view of landing trajectory. Circles and crosses represent the centre of the rotor for that particular test condition.

To investigate the effect of wind velocity and direction, the experiment has been carried out in both windy and not windy conditions, for two different wind directions, i.e. headwind (β = 0°) and Red-30 (β = 30°, port side). However, for the purpose of this paper only the database of headwind condition will be presented and analyzed. The chosen wind speed of 4.8 m/s corresponds to a full-scale velocity of 20 kt and to an advance ratio $\mu = U_{\infty}/V_{TIP} = 0.047$. Load measurements in headwind condition for both horizontal and vertical trajectories are presented in the last section in comparison with simulation results.

3 MULTIBODY MODELLING

A multibody model of the experimental rotor has been developed using MBDyn which is a free general-purpose multibody dynamics analysis software [13]. MBDyn features the integrated multidisciplinary simulation of multibody systems, including nonlinear mechanics of rigid and flexible bodies subjected to kinematic constraints, along with smart materials, electric and hydraulic networks, active control and essential elements of rotorcraft aerodynamics [14]. The multibody model developed for this study consists of four elastic blades connected to the hub by implementing a revolute hinge which allows only rotation around the feathering axis of the blade. This degree of freedom along with a rigid pitch link connected to the swashplate allow us to apply the pitch control. To be consistent with the experimental rotor, no flapping and lead-lag hinges are implemented in the model. However, flapping motion has been modeled considering the out of plane stiffness of the elastic beams which are representing the blade. Eigenanalysis of the model in vacuum shows that the flapping frequency at nominal rotor speed is 22 percent higher than frequency of the rotor, ν_{β}=1.22 /rev. In the following section, Fan-Plot of the flapping mode, which shows the variation of the natural flapping frequency in different rotor speeds will be compared with those obtained by the linearized model. The parameters of the model are summarized in 1.

The aerodynamic characteristics of the blade has been modeled using NACA0012 as the airfoil, considering 3 percent of aerodynamic tip loss at the blade tip. Moreover, ground effect has been incorporated into the simulation based on the model presented in [15].

Fradenburgh conducted ground effect test using a two-bladed rotor with diameter of D=2 ft, operating at tip-speed of approximately 600 ft/sec. The results show that the thrust is increased by 15 percent when the rotor moves toward the ground from 3R to 1R. Similar results were obtained in the experimental wind tunnel tests performed at GVPM.

As mentioned before, the current experiment does not represent a dynamic manoeuvre, which means that the load measurements are related to the steady response of the rotor. So, at this stage, dynamic inflow is not implemented into the simulation environment and the induced velocity has been modelled using a static model which has a linear distribution over the rotor disk [16]:

$$v_i = v_0(1 + \kappa_x r \cos\psi + \kappa_y r \sin\psi) \tag{2}$$

The classical vortex theory results give estimates of the factors κ_x and κ_y. Drees suggested following equations to approximate the linear variation of the inflow [16]:

$$\kappa_x = f_x\,(4/3)(1 - \cos\chi - 1.8\,\mu^2)\ ,\ \kappa_y = f_y(-2\mu) \tag{3}$$

Here, f_x and f_y are empirical factors that are incorporated in each of the above equations to modify the inflow distribution in both lateral and longitudinal directions (f_x=f_y=1 in Drees model) [17]. These factors have been set in order to generate same load coefficients, including thrust, torque and in-plane moments, while rotorcraft is positioned in the initial point of the landing trajectory (P1).

Number of Blades	4
Rotor Radius (m)	0.375
Angular Velocity (rad/s)	270.17
Blade Chord (m)	0.032
Free Stream Velocity	4.93
Advanced Ratio	0.048
Tip Mach Number	0.3
Tip Reynolds Number	220000

Table 1: Parameters of the rotor model.

4 IDENTIFICATION ALGORITHM

Looking at the results of the load measurements while rotorcraft approaching the flight deck (Figure 3, 4), it can be seen that the velocity field above the rotor should be modified in order to get the same loads as the experiment for the whole landing trajectory. Considering the long-term goal of this project, which has been explained in the introduction part, the velocity measurements cannot be implemented directly in the simulation environment. Consequently, an optimization algorithm has been developed in order to find the external gust component to reproduce the same loads. Further adjustment of the inflow empirical factors has been considered in order to slightly modify the contribution of lateral and longitudinal moments, if needed.

Gust velocity is considered to have a linear distribution in radial and azimuthal direction (similar to inflow), so it can be defined as the following equation:

$$V_g = V_{g0} + V_{gc} r \cos\psi + V_{gs} r \sin\psi) \tag{4}$$

Then, the optimization procedure has been done taking two steps as follows:

- Finding a constant gust velocity to match the thrust coefficient, considering the following cost function:

$$MIN(J) \quad with \quad J = \sqrt{(C_t - C_{t_{exp}})^2} \tag{5}$$

- finding the first harmonics of gust velocity to generate same moment coefficients. Considering the following cost function:

$$MIN(J) \quad with \quad J = \sqrt{\left(\frac{C_m - C_{m_{exp}}}{C_{m_{exp}}}\right)^2 + \left(\frac{C_l - C_{l_{exp}}}{C_{l_{exp}}}\right)^2} \tag{6}$$

It should be noted that since the ground effect has been implemented in the simulation, the variation of thrust is mainly caused by the altitude change. However, a small constant gust can be added to improve the matching.

5 RESULTS AND DISCUSSION

The simulation results implementing the solution of optimization algorithm as an external gust, are compared with the load measurements in headwind condition for all points along the landing and vertical trajectory. Figure 3.a compares the load coefficients for 5 points of the landing trajectory (P1 to P5). Horizontal axis refers to the same coordinate system shown in Figure 2. It should be noted that all the results are presented in rotor reference frame, as defined in Figure 2.

Regarding the experimental results, as it is expected, the thrust coefficient is increasing while rotorcraft approaching the landing point, since it enters the ground effect of the flight deck. The presence of the external wind also results in pitch and roll moments on the rotor. Due to the combination of the wind velocity and rotational velocity of the rotor, asymmetric thrust is generated in advancing and retreating side of the rotor plane, which produces a positive roll moment (roll to left). Considering the stiffness of the rotor, roll moment produces a positive pitch moment (nose up) by tilting the vector of the angular momentum in backward direction. This is also related to the distribution of the induced velocity in forward flight which results in reduced inflow in fore part and increased inflow in the aft part of the rotor.

As it can be seen, the simulation results are highly consistent with the measurements which means the external gust is well representative of the environmental effects on rotor performance. There is an offset of 25% in torque coefficient that could be related to a higher profile drag of airfoil given the different Reynolds number and the additional drag of the inner part of the rotor in experiment compared with simulation in which there is no aerodynamic contribution for the hub.

Figure 3.b refers to the same comparison for the vertical trajectory (P5 to P8). Here, horizontal axis refers to the rotor altitude from the flight deck as it has been shown in Figure 2. It is notable that in the landing point, which is 0.8R above the flight deck, the rotor is completely immersed in the ground effect and wake of the hangar wall. Similar to the previous results, as the rotorcraft is going upward, thrust is decreasing and in plane moments are getting closer to the initial point of the landing in which the rotor is less affected by the ship airwake.

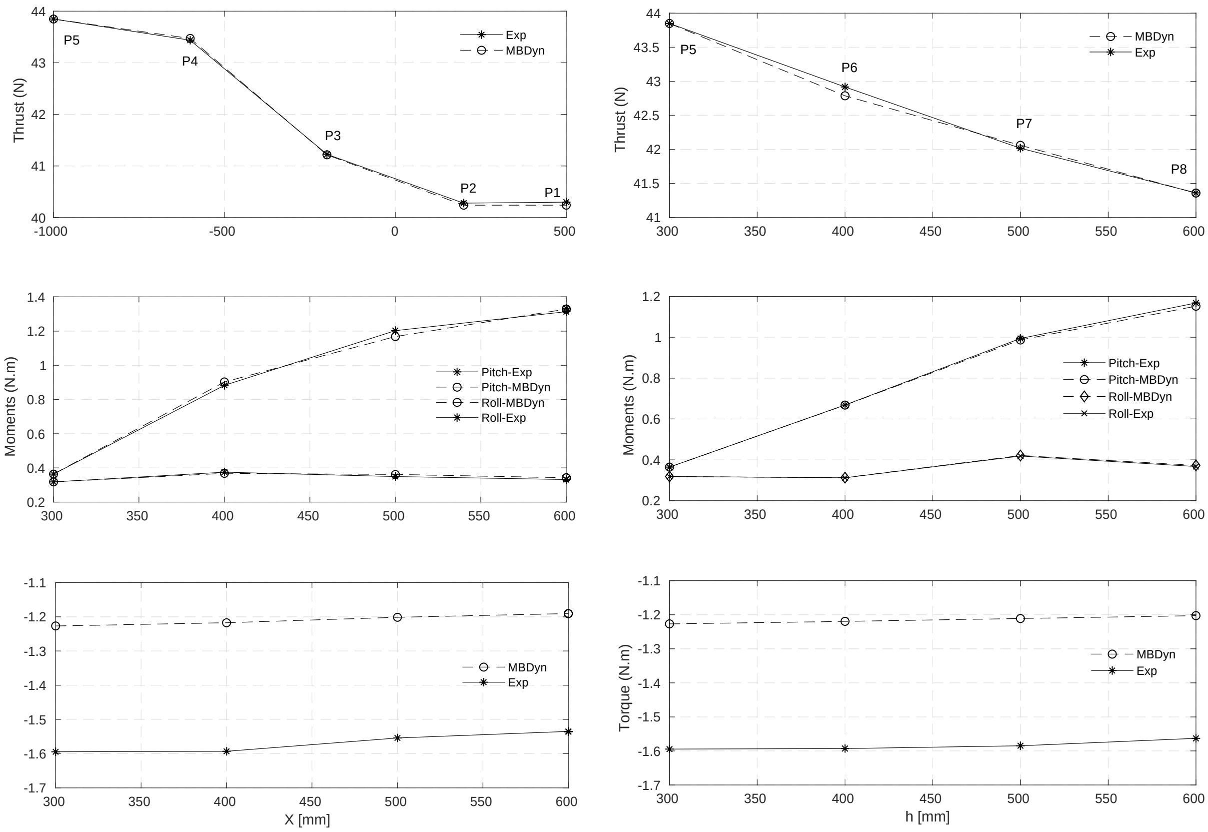

Figure 3: Comparison of loads from simulation and experiment. (a): Horizontal trajectory (b): Vertical Trajectory

To be more clear, the first harmonics of the gust are compared for all test points (Figure 4). The results show that initial points of the landing (P1 and P2) do not need additional modification of the velocity field. However, moving towards the landing point, the amplitude of the gust will be larger, which is consistent with the variation of the moment coefficients.

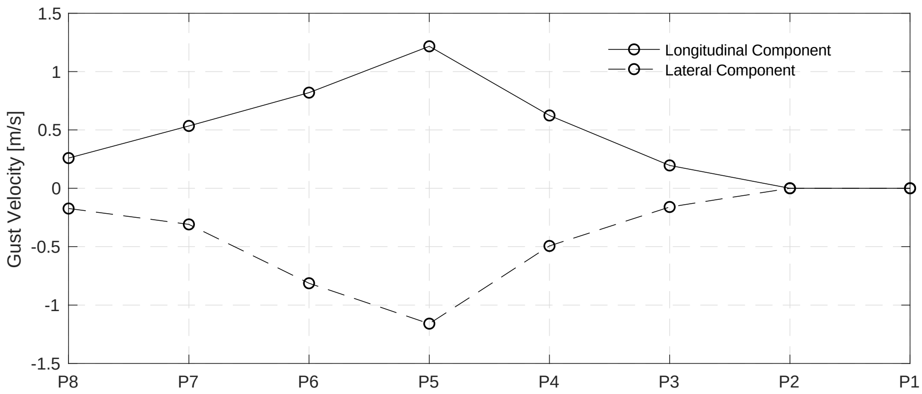

Figure 4: Lateral and longitudinal components of identified gust for all test points.

6 CONCLUDING REMARKS

This work investigated the aerodynamic interaction between a scaled-down helicopter and simplified ship geometry in order to develop a gust identification algorithm to be incorporated into the simulation environment to model the environmental effect on the rotor performance. To this aim, a series of wind tunnel experiment has been performed to simulate a typical fore-aft landing trajectory on the flight deck. A multibody model of the rotor has been developed in MBDyn for simulation purpose. A linear distribution of the inflow has been implemented, however, it has been modified with empirical factors in order to generate same load coefficients as the experiment at starting point of the landing manoeuvre. This model has been further modified by introducing a gust element into the model, while rotorcraft approaching the flight deck. The gust velocity is identified through an optimization algorithm with the objective of generating same in-plane moments as the experiment. Comparison of the results with experimental data shows that the gust element can modify the inflow of the rotor so that producing same loads in the presence of aerodynamic interaction. In the future, this approach will be implemented in a closed-loop communication between full-scale flight simulator and small-scale test setup in the wind tunnel.

7 ACKNOWLEDGEMENTS

The project NITROS (Network for Innovative Training on ROtorcraft Safety) has received funding from the European Union’s Horizon 2020 research and innovation program under the Marie Sklodowska-Curie grant agreement No. 721920.

REFERENCES

[1] Hodge, S. J., Zan, S. J., Roper, D. M., Padfield, G. D., and Owen, I., “Time-Accurate Ship Airwake and Unsteady Aerodynamic Loads Modeling for Maritime Helicopter Simulation”, *Journal of American Helicopter Society*, **Vol. 54, (2)**, pp. 1-16, April (2009).

[2] Owen, I., White, M. D., Padfield, G. D., and Hodge, S. J., “A virtual engineering approach to the ship-helicopter dynamic interface¸ a decade of modelling and simulation research at the University of Liverpool”, *The Aeronautical Journal*, **Vol. 121, (1246)**, pp. 1833–1857, December (2017).

[3] Quaranta, G., Barakos, G., White, M., Pavel, M., and Mulder, M., “NITROS: An Innovative Training Program to Enhance Rotorcraft Safety,” American Helicopter Society International 74th Annual Forum, Phoenix, USA, May (2018).

[4] Kaaria, C. H., Forrest, J. S., Owen, I., and Padfield, G. D., “Simulated aerodynamic loading of an SH-60B helicopter in a ship’s airwake,” 35th European Rotorcraft Forum, Hamburg, Germany, September (2009).

[5] Chirico, G., Szubert, D., Vigevano, L., and Barakos, G. N., “Numerical modelling of the aerodynamic interference between helicopter and ground obstacles”, *CEAS Aeronautical Journal*, Vol. 8, (4), pp. 589–611, December (2017).

[6] Bludau, J., Rauleder, J., Friedmann, L., and Hajek, M., “Real-Time Simulation of Dynamic Inflow Using Rotorcraft Flight Dynamics Coupled with a Lattice-Boltzmann Based Fluid Simulation”, 55th AIAA Aerospace Sciences Meeting, AIAA SciTech Forum, Grapevine, Texas, January (2017).

[7] Oruc, I. and Horn, J. F., "Coupled Flight Dynamics and Computational Fluid Dynamics Simulations of Rotorcraft/Terrain Interactions", *Journal of Aircraft*, **Vol. 54, (6)**, pp. 2228–2241, June (2017).

[8] Crozen, C., Steijl, R., and Barakos G. N., "Coupled flight dynamics and CFD demonstration for helicopters in shipborne environment", *The Aeronautical Journal*, **Vol. 122, (1247)**, pp. 42–82, January (2018).

[9] Reddy, K. R., Toffoletto, R., and Jones, K. R., "Numerical simulation of ship airwake", *Computers and fluids*, **Vol. 29, (4)**, pp. 451–465, May (2000).

[10] Gibertini, G., Gasparini, L., and Zasso, A., "Aerodynamic design of a civil-aeronautical low speed large wind tunnel", AGARD 79th fluid dynamics panel symposium, Moscow, Russia, January (1996).

[11] Zagaglia, D., Zanotti, A., and Gibertini, G., "Analysis of the loads acting on the rotor of a helicopter model close to an obstacle in moderate windy condition", *Aerospace Science and Technology*, **Vol. 78**, pp. 580–592, (2018).

[12] Gibertini, G., Grassi, D., Parolini, C., Zagaglia, D., and Zanotti, A., "Experimental investigation on the aerodynamic interaction between a helicopter and ground obstacles", *Proceedings of the Institution of Mechanical Engineers, Part G: Journal of Aerospace Engineering*, **Vol. 229, (8)**, pp. 1395–1406, (2015).

[13] Masarati, P., Morandini, M., and Mantegazza, P., "An efficient formulation for general-purpose multibody/multiphysics analysis", *ASME Journal of Computational Nonlinear Dynamics*, **Vol. 9, (4)**, pp. 041001–041001–9, July (2014).

[14] Masarati, P., Piatak, D. J., Quaranta, G., Singleton, J. D., and Shen, J., "Soft In-plane Tiltrotor Aeromechanics Investigation Using Two Comprehensive Multibody Solvers", *Journal of the American Helicopter Society*, **Vol. 53, (2)**, pp. 179–192, (2008).

[15] Fradenburgh, E. A., "The helicopter and the ground effect machine", *Journal of the American Helicopter Society*, **Vol. 5, (4)**, pp. 24–33, October (1960).

[16] Johnson, W., "Rotorcraft Aeromechanics", Cambridge University Press, first edition, Chapter 5, p. 136, (2013).

[17] Johnson, W., "CAMRAD/JA, A Comprehensive analytical model of rotorcraft aerodynamics and dynamics-Volume I: Theory manual, Johnson Aeronautics Version", (1988).